

Persistent revivals in a system of trapped bosonic atoms

Carlos Diaz Mejia^a, Javier de la Cruz^a, Sergio Lerma-Hernández^b, Jorge G. Hirsch^a

^a*Instituto de Ciencias Nucleares, Universidad Nacional Autónoma de México, Apdo. Postal 70-543, 04510, CDMX, Mexico*

^b*Facultad de Física, Universidad Veracruzana, Campus Arco Sur, Paseo 112, 91097, Xalapa, Mexico*

Abstract

Dynamical signatures of quantum chaos are observed in the survival probability of different initial states, in a system of cold atoms trapped in a linear chain with site noise and open boundary conditions. It is shown that chaos is present in the region of small disorder, at intermediate energies. The study is performed with different number of sites and atoms: 7,8 and 9, but focusing on the case where the particle density is one. States of the occupation basis with energies in the chaotic region are evolved at long times.

Remarkable differences in the behaviour of the survival probability are found for states with different energy-eigenbasis participation ratio (PR). Whereas those with large PR clearly exhibit the characteristic random-matrix correlation hole before equilibration, those with small PR present a marginal or even no correlation hole which is replaced by revivals lasting up to the stage of equilibration, suggesting a connection with the quantum scarring phenomenon.

Keywords: trapped atoms, quantum chaos, survival probability.

Email addresses: carlosdime@estudiantes.fisica.unam.mx (Carlos Diaz Mejia), javierdelacruz@ciencias.unam.mx (Javier de la Cruz), slerma@uv.mx (Sergio Lerma-Hernández), hirsch@nucleares.unam.mx (Jorge G. Hirsch)

1. Introduction

Quantum chaos is a concept closely related to and deeply rooted in Random Matrix Theory (RMT), a formalism useful to describe the correlations in the spectrum of a quantum system with a classical correspondent that is chaotic [1, 2]. RMT also provides the mathematical framework to support the Eigenstate Thermalization Hypothesis (ETH) [3, 4], which explains the thermalization of quantum many-body system by using a small set of chaotic eigenstates around a given energy, expected to have similar properties. In the description of chaos and thermalization the focus is on the properties of the eigenvalues and eigenvectors of the Hamiltonian. The dynamics of a given initial state centered in the same energy region is strongly influenced by these spectral properties, but its particular structure plays also a relevant role. To what extent the properties of the initial state are important for the different temporal scales in their dynamics? In which cases the dynamics is determined solely by the universal properties coming from RMT? In what follows we address these questions for a system of trapped atoms and a set of experimentally relevant initial states.

Experiments and numerical simulations in the Interacting Aubry-Andre model (IAA), consisting of eight bosons and eight sites [5], have explored the presence of thermalization. The central observable was the entanglement entropy of one site with the rest at long times, for an initial Mott state with one boson per site. The study showed the presence of thermalization for weak disorder, and that, for a large disorder parameter, the relaxation value of the entanglement entropy did not match the expected thermal average provided by the ETH. This phenomenology is attributed to many-body localization (MBL)[6], where non-local correlations would not persist during the evolution of the observable.

A different manifestation of weak ergodicity breaking is the existence of persistent revivals of observables[7]. Typically, they occur when ETH and quantum chaos are valid. Since the discovery of this oscillatory phenomena in Rydberg chains[8, 9], many experiments and theoretical[10] studies have arisen to extend the research on quantum scars. Some examples are: Hubbard models[11, 12], spin chains [13, 14] and quantum simulators[12, 15], etc. There are still some open questions regarding why there are some states that only explore a small set of a very large Hilbert space.

In this work, our central results focus on the chaotic region, where ETH is valid, and even so, some initial states do not evolve as expected according to RMT. We present a detailed study of the quantum dynamical properties of the Interacting Aubry-André model for a set of occupation (Fock) initial states. We performed a scaling analysis from 7 bosons and 7 sites up to 9 bosons and 9 sites, which have Hilbert-space dimensions, $\dim = \binom{2N-1}{N-1}$, from 1716 up to 24310, and confirmed that the chaotic (RMT) correlations in the spectrum remain at the same interval of energy per particle.

A classification of all the possible initial states on the site basis is developed introducing a crowding parameter, which is correlated with the expectation value of the energy of the occupation states, averaged over different realizations of the Hamiltonian. It is shown that the states whose energies lie in the chaotic region have larger participation ratios (PR) in the eigenbasis than those in the regular region, which have PR noticeably smaller. The states with the largest PR in the chaotic region exhibit the so-called correlation hole in their survival probability, while the states with the smallest PR in the same chaotic region, have a survival probability not showing such correlation hole and have lasting revivals persisting

up to the equilibration stage of their evolution.

The structure of the paper is as follows: in section 2 we introduce the Hamiltonian of the system with emphasis on the energy level spacing ratio to determine the values of the disorder parameter and the energies where quantum chaos is present, in section 3 the states in the occupation basis are classified according to the crowding parameter and Participation Ratio in the Hamiltonian eigenbasis. In section 4 we analyze the survival probability of the occupation states, and the presence or absence of the correlation hole, which is the hallmark of chaotic dynamics. Conclusions are presented in section 5. In the Appendix some technical aspects of the evaluation of the Survival Probability are presented.

2. The Interacting Aubry-André model (IAA) and spectral signatures of quantum chaos

The Interacting Aubry-André model (IAA) describes the dynamics of N spin-less bosons on a lattice with L sites in a one dimensional chain[16]. The corresponding Hamiltonian($\hbar = 1$) is

$$H = -J \sum_{\langle i,j \rangle} \hat{b}_i^\dagger \hat{b}_j + \frac{U}{2} \sum_i \hat{n}_i(\hat{n}_i - 1) + W \sum_i \cos(2\pi\beta i + \phi) \hat{n}_i, \quad (1)$$

where \hat{b}_i^\dagger and \hat{b}_i are the bosonic creation and annihilation operators on the site i . The first term describes the tunneling between neighboring lattice sites with rate J . The second term represents the energy shift U when multiple particles occupy the same site, with $\hat{n}_i = \hat{b}_i^\dagger \hat{b}_i$ the number of particles on site i . The last term introduces a site-resolved potential offset, which is created with an incommensurate lattice $\cos(2\pi\beta i + \phi)$ of period β lattice sites, phase ϕ , and amplitude W , known as disorder parameter. The Hamiltonian parameters J , U , W and ϕ can be controlled in the

experiment [5]. In our study the phase ϕ varies randomly from one realization to another in order to make clearer the spectrum correlations in the observable we considered.

For large values of the disorder parameter W in Hamiltonian (1) many-body localization (MBL) breaks thermalization; particles are localized and transport ceases. This localization transition is very sensitive to the value of the parameter β , which is selected as an incommensurate number, the ratio of two prime numbers $\beta = P/Q$. In the experiment it is related with the two laser wavelengths. In this work the values $\beta = 1.618$ [5], $U = 4/(N - 1)$ and $J = 1/2$ are employed in the calculations. The parameter U is scaled by factor $1/(N - 1)$ in order to obtain the same scaling properties for all the terms in the Hamiltonian. The latter values are associated with the presence of chaos when $W = 0$ [17, 18, 19].

In what follows, a spectral analysis is presented by exact diagonalization, based on averages over 40 numerical random realizations of the phase ϕ in the range $[0, 2\pi]$ [20].

A widely employed signature of quantum chaos relates properties of the energy spectrum with those of random matrices [21]. Given an ordered set of eigenenergies E_n , with $n = 1, 2, \dots, d$, the nearest-neighbor spacing is given by $s_n = E_{n+1} - E_n$. Quantum chaotic systems have level spacing described by the Wigner-Dyson distribution, characterized by level repulsion. In the Gaussian Orthogonal Ensemble (GOE) it reads

$$P(\tilde{s}) = \frac{\tilde{s}}{2\sigma^2} e^{-\tilde{s}^2/4\sigma^2}, \quad (2)$$

in terms of the unfolded variable $\tilde{s} = s/\Delta E$, being $1/\Delta E$ the density of states.

On the other hand, in regular systems, with non-correlated eigenvalues, the distribution of level spacing is well described by

the Poisson distribution.

$$p(\tilde{s}) = e^{-\tilde{s}}. \quad (3)$$

To avoid the complication of the unfolding, in this work we employ the ratio of two consecutive level spacings proposed by Oganesyan and Huse[22, 23, 24].

$$r_n = \frac{\min(s_n, s_{n-1})}{\max(s_n, s_{n-1})} \quad (4)$$

This quantity is independent of the density of states and no unfolding is necessary. For quantum chaotic systems, the distribution of the level spacing ratio has an average of [25, 26]

$$\tilde{r}_W = 4 - 2\sqrt{3} \approx 0.535, \quad (5)$$

while for regular systems, it has a lower value of

$$\tilde{r}_P = 2 \ln 2 - 1 \approx 0.386. \quad (6)$$

2.1. The disorder parameter and chaos

The level spacing ratio of Hamiltonian (1) is depicted in Fig. 1 as a function of the disorder parameter W for $N = L = [7, 8, 9]$ bosons and sites, and also for $L = 8$ sites and $N = L \pm 2$ bosons, in a linear chain with open boundary conditions. It is clear that chaos is present in the region $W \leq 1$ for all the cases considered. A closer view of this region in the inset shows that the presence of chaos remains at the same interval of W irrespective of the number of sites and density. In this paper, the value $W = 0.6$, at the middle of this region, is selected to study the chaotic dynamics. It is worth mentioning that we have excluded the case $W = 0$ from the figures, since in this case the Bose-Hubbard model presents invariant subspaces that require a differentiated analysis of the level-spacing ratios in each subspace [19].

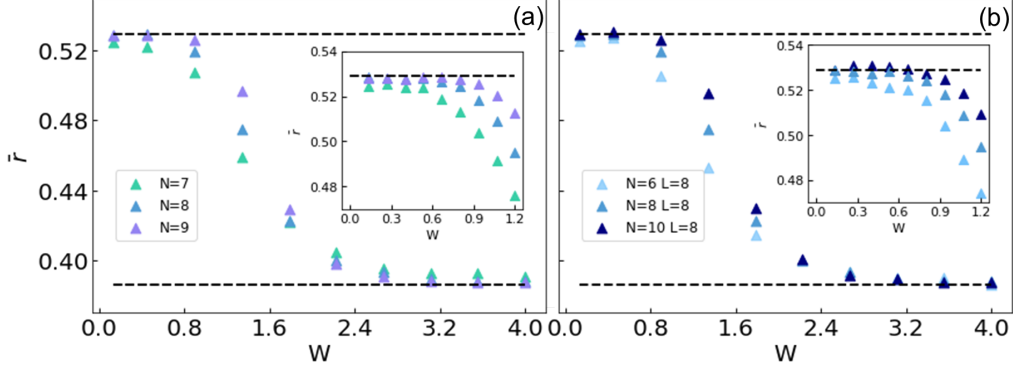


Figure 1: Average of two consecutive level spacing ratios as function of the disorder parameter W for (a) $N = L \in [7, 8, 9]$ and $W \in [0, 4]$, (b) for different particle densities, $N = L \pm 2$, $L = 8$. Insets, zoom for $W \in [0, 1.2]$. Only the 80 % of the central part of the spectra was considered, by neglecting the 10 % lowest and 10 % highest energy levels of the spectra. The upper and lower dashed lines show the limits $\tilde{r} = 0.53$, and $\tilde{r} = 0.38$.

2.2. Chaos and regularity in presence of weak disorder

In Fig. 2 (a) a refined analysis of regularity and chaos is presented, employing the level spacing ratio for the case of weak disorder $W = 0.6$. Averages are made over 40 realizations of the Hamiltonian with different, randomly selected, disorder phases ϕ , allowing to have enough statistics (around 500 energy level spacings) in small energy intervals centered at different energies. The dots represent the value \tilde{r} for the energy levels in the intervals plotted versus the mean energy of the levels in those intervals. The figure shows that the chaotic region in the energy spectrum lies approximately in the interval $E/N = [-0.4, 1.0]$. As expected, at upper energy regions the quantum dynamics are regular. In Fig. 2 (b), the histogram of the density of states (DOS) is presented for the three different system sizes considered, showing a similar behaviour in terms of the scaled energy.

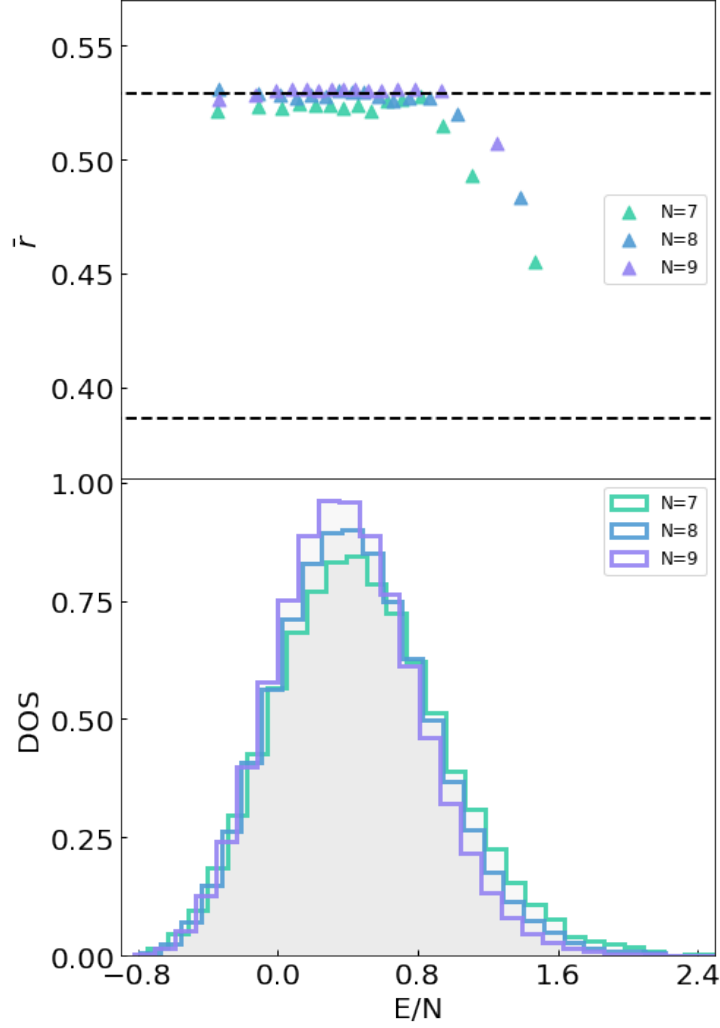


Figure 2: (a) The level spacing ratio is shown for different sets of the same number of consecutive states, for $W = 0.6$. The upper and lower dashed lines show the limits $\tilde{r} = 0.53$, and $\tilde{r} = 0.38$. (b) In shaded gray the DOS histogram is shown. Both figures represent $N = L \in [7, 8, 9]$.

3. Classification of the occupation states and Participation Ratio

As mentioned before, in Ref. [5] evidence of ETH was observed for weak values of the disorder parameter. In that reference the authors considered as initial state one atom in each site (the Mott state), which is a particular state of the occupation or Fock basis. In order to address possible deviations of this behaviour for other experimentally accessible initial states, we consider in this study the whole set elements in the Fock basis as initial states. This set covers an ample range of energies, both in the chaotic and regular regime of the spectrum and, as shown below it presents a great diversity of behaviours which make it an adequate set to sample a generic initial state, even those with an initial entanglement between sites. This latter statement comes from the fact that the chaotic properties of the model makes that non initially entangled states, as those of the Fock basis, become entangled after a transient temporal interval.

The Fock basis is defined as

$$|k\rangle = |n_1, n_2, \dots, n_L\rangle, \quad (7)$$

with L the number of sites, and

$$\sum_{i=1}^L n_i = N, \quad (8)$$

where N is the total number of atoms in the system. In this work we also use weak values of the disorder parameter ($W = 0.6$) for three different sizes $N = L \in [7, 8, 9]$, allowing us to perform a scaling analysis of our results.

In order to classify the states of the Fock basis and select those more adequate for our study, we consider several quantities. The

first one is their mean energy per particle $E_k/N = \langle k|H|k\rangle/N$. The second quantity used in this classification is the Participation Ratio (PR) respect to the Hamiltonian eigenbasis. The PR provides an effective estimation of the number of states of a given basis $\{|m\rangle\}$ (the Hamiltonian eigenbasis in this case), which are needed to build a given state $|k\rangle = \sum_m c_m^k |m\rangle$. It is defined as

$$\text{PR}(k) = \frac{1}{\sum_m |c_m^k|^4}. \quad (9)$$

The largest the PR, the more delocalized is the state in this basis. In first row of Fig. 3 we show the PR divided by the dimension (dim) of the respective Hilbert space versus E_k/N for all the states of the Fock basis in the three system sizes considered. While the eigenenergies range between $E/N = -0.8$ and $E/N = 2.4$, the mean energies per particle of the occupation states are more concentrated, with most of them having energies between 0 and 1. Note that most of the states in the occupation basis have mean energies in the middle of the spectrum which is chaotic according to Fig.2. Additionally, observe that the states are organized in several clusters with approximately the same energy. The cluster with lowest energy consists of only one state, the Mott state with one particle per site. The different clusters can be labeled by the *crowding parameter*

$$C = \frac{1}{N} \sum n_i^2, \quad (10)$$

which ranges from 1, for the Mott state to N when all the particles are located in only one site. Observe that, since the hopping term in (1) has no diagonal components in the occupation basis, and the disorder term is an oscillatory function of the phase ϕ with null average over many realizations, the average energy of the occupation states has only contributions from the interaction

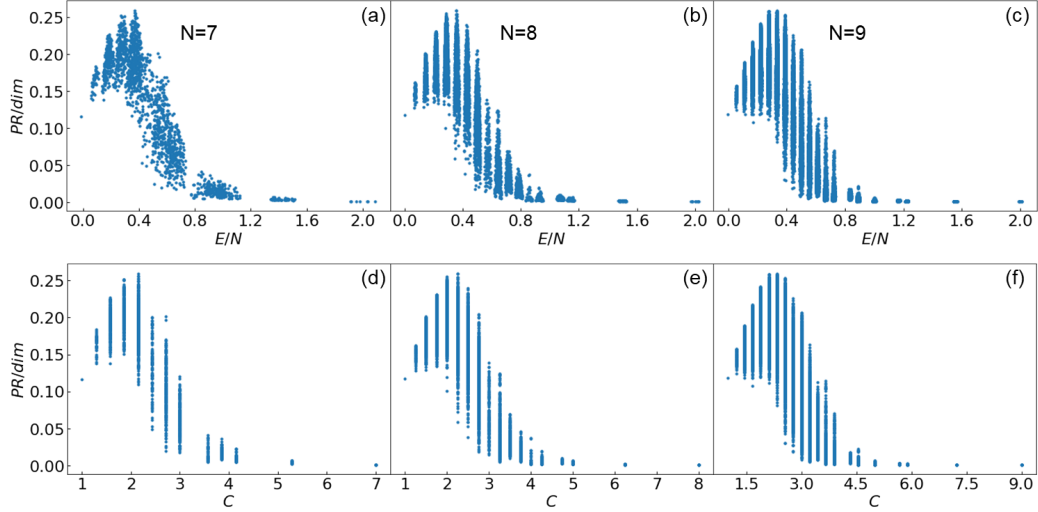


Figure 3: (a)-(c) PR/dim vs E/N for all occupation states, (d)-(f) PR/dim vs C , each column corresponds to different scale from $N = 7$ to $N = 9$.

term [the second one in the Hamiltonian of Eq. (1)]. For this reason, the average value of the energy is approximately linear in the crowding parameter $E_k/N = U(C - 1)/2$.

Second row of Fig. 3 presents the same ratio PR/dim of all occupation states plotted against their crowding parameter. Note that the clusters of energy become vertical lines, facilitating the classification of the states. It can be seen that most of the states, whose C lie between 1 and 2.5 have the largest PR and $E_k/N < 1$. On the other hand, those states with larger C have highest energies and lowest PR values. Therefore, in general terms, states with small C are less localized in the Hamiltonian eigenbasis than those with larger C , which are far more localized. Nevertheless, observe that the states with small C have a considerable dispersion in their PR values. For instance, for states with $C \approx 2$ the ratio PR/dim ranges approximately from 0.1 up to 0.25.

In the next section we study the dynamics of initial Fock states

with a crowding parameter $C \sim 2$ which have a mean energy per particle well inside the chaotic region of the spectrum. We consider the three different system sizes and for a given C we select states with high and low PR in order to detect differences in their dynamics. The dynamical quantity we choose to perform our study is the survival probability, whose definition and properties are discussed in the following section.

4. The Survival probability and the correlation hole

The survival probability $S_P(t)$ is defined as the probability to find any initial state $|\Psi(0)\rangle$ after an evolution with time t ,

$$S_P(t) = |\langle \Psi(0) | \Psi(t) \rangle|^2 = \left| \sum_m |c_m|^2 e^{-iE_m t} \right|^2, \quad (11)$$

c_m are the components of the initial state in the Hamiltonian eigenbasis, $|\Psi(0)\rangle = \sum_m c_m |E_m\rangle$. The survival probability is closely related to the spectral form factor (SFF) [27], which is the survival probability of an initial state whose components are given by a Gibbs thermal distribution $|c_m|^2 = \frac{e^{-\beta E_m}}{Z(\beta)}$ with $Z(\beta) = \sum_m e^{-\beta E_m} = \text{Tr } e^{-\beta H}$.

The survival probability (SP) has been used in recent works as a quantum indicator of chaos, partly because for random initial states there exists an analytical expression that relates the two-level form factor of GOE full random matrices with the dynamics of the survival probability at long times [28, 29, 30, 31, 32, 33, 34, 19]. This implies that at long temporal scales the behavior of this observable is universal, i.e. it is dictated by the same spectral correlations as those of gaussian ensembles of random matrices. From an experimental point of view, the SP can detect chaos without the need and complications of measuring the complete set

of eigenenergies. Additionally, the SP can detect quantum chaos even if there are some hidden symmetries [19], which is a limitation of nearest-neighbor spacing distributions that are strongly affected by hidden symmetries in the models.

If there are no degeneracies[19, 35], the temporal average of the survival probability at long times approaches the Inverse Participation Ratio

$$\langle S_P^\infty \rangle = \text{IPR} = \sum_m |c_m|^4. \quad (12)$$

It is the inverse of the PR of Eq. 9, which provides an estimation of the number of elements of a given basis (the energy eigenbasis, in this case) participating in an arbitrary quantum state.

Random matrix theory allows to obtain an analytical expression for the survival probability of an ensemble of random states with a given smoothed local density of states $\rho(E)$ (see below) and energy components in the chaotic region of the spectrum characterized by level correlations of the Gaussian orthogonal ensemble (GOE). It reads [34, 36, 19, 28, 29, 30, 32]

$$\langle S_P(t) \rangle = \frac{1 - \text{IPR}}{\eta - 1} \left[\eta S_P^{bc}(t) - b_2 \left(\frac{t}{2\pi\bar{\nu}} \right) \right] + \text{IPR}, \quad (13)$$

where $S_P^{bc}(t)$ is given by the Fourier transform of the smoothed Local Density of States as

$$S_P^{bc} = \left| \int \rho(E) e^{-iEt} dE \right|^2, \quad (14)$$

the mean density of states $\bar{\nu}$ is taken in the energy region where the components c_m are more important, and the parameter η takes into account the availability of energy levels,

$$\eta = \frac{1}{\int dE \frac{\rho^2(E)}{\nu(E)}}. \quad (15)$$

The details of the estimation of this parameter are explained in Appendix A.

For a given state, the local density of states (LDoS) is defined as

$$\rho_L(E) = \sum_m |c_m|^2 \delta(E - E_m). \quad (16)$$

A smoothed local density of states $\rho(E)$ can be obtained from the components of the initial state by fitting a continuous distribution to the histogram

$$\rho(\mathcal{E}_i) = \sum_{\substack{m \text{ with} \\ |\mathcal{E}_i - E_m| < \Delta\mathcal{E}/2}} |c_m|^2,$$

for a set of equally spaced energy values $\mathcal{E}_{i+1} - \mathcal{E}_i = \Delta\mathcal{E}$. The value $\Delta\mathcal{E}$ determines the degree of resolution with which $\rho(E)$ describes the LDoS, $\rho_L(E)$. For $\Delta\mathcal{E}$ less than the difference of consecutive levels we obtain maximal resolution, whereas for $\Delta\mathcal{E} \sim \Delta H$ we obtain a smoothed $\rho(E)$ which determines the initial decay of the survival probability in Eq.(13). In Fig.4(c) we show this smoothing of the LDoS for a representative initial state, for which we fitted a Gaussian distribution. The next term in Eq. (13) is the two-level form factor of the GOE ensemble [28],

$$b_2(t) = [1 - 2t + t \ln(2t + 1)] \Theta(1 - t) + \left[t \ln \left(\frac{2t + 1}{2t - 1} \right) - 1 \right] \Theta(t - 1), \quad (17)$$

where Θ is the Heaviside step function. The two-level form factor evolves the survival probability from a minimum to its relaxation value $\langle S_P^\infty \rangle$, performing a dip known as the *correlation hole*. As mentioned above, for a given initial state in the occupation basis we consider 40 realizations of the Hamiltonian. For each realization we calculate numerically the survival probability and, at each time, we consider its average over the realizations. By using the

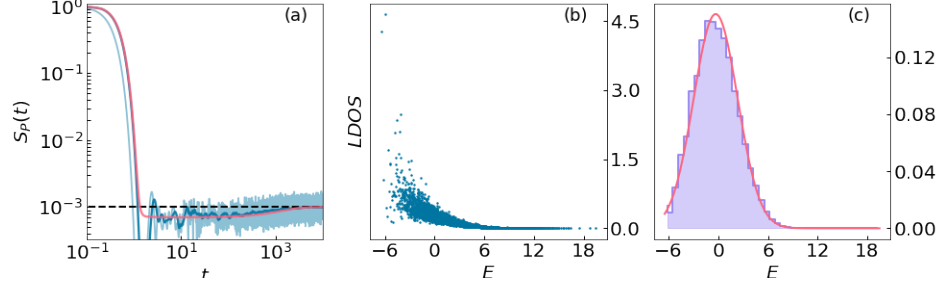


Figure 4: (a) Survival probability for the Mott ($N = L = 8$) state $|\Psi(0)\rangle = |1, 1, \dots, 1\rangle$, (b) the LDoS ($\times 10^{-3}$) and (c) the smoothed LDoS histogram for constant windows of energy $\Delta E = 0.74$ for only one realization in ϕ , in red the Gaussian fit.

Mott state, an illustrative result of this procedure is shown by the light curve in Fig.4(a). We see that, after the initial decay, the averaged survival probability displays temporal oscillations. In order to smooth these quantum fluctuations, we consider additionally a temporal rolling average, which is shown in the same figure by a dark blue line. This rolling temporal average makes more evident the presence of a hole in the survival probability, described by Eq. (13) (red line in the figure), which is a direct signature of the existence of correlated eigenvalues. The red line in Fig.4(a) was obtained by considering a Gaussian fit to the smoothed LDoS of Fig.4(c). The LDoS at full resolution is shown in Fig.4(b). It is worth mentioning that the correlation hole does not appear in systems with uncorrelated eigenvalues, which is not the case of the Mott initial state of Fig.4,

4.1. Numerical results

We focus, for the three different system sizes, on initial states of the Fock basis with a mean energy inside the already identified chaotic region and study their survival probabilities. For that, for each system size, we select, as representative of the diverse

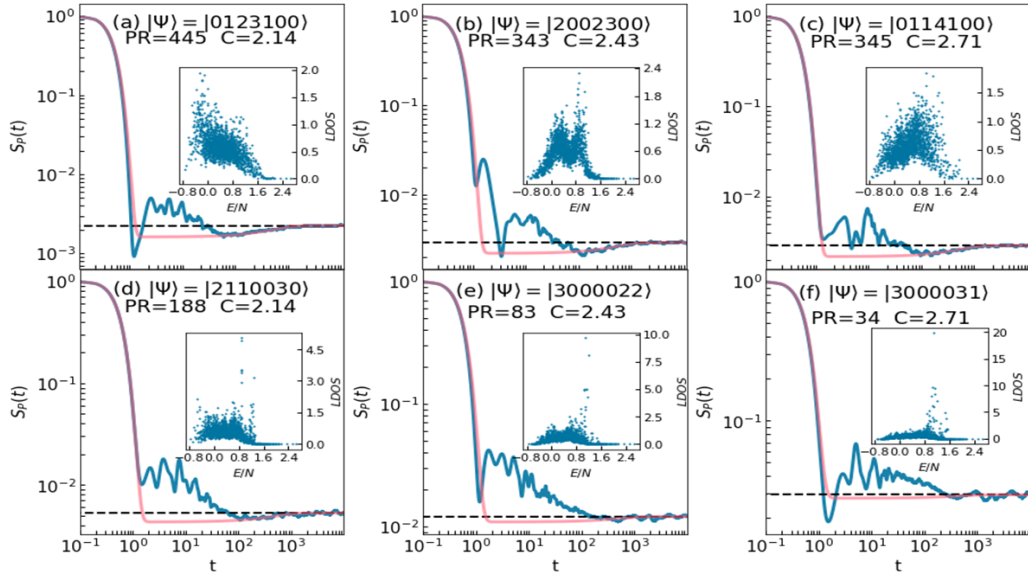


Figure 5: Survival probability of selected states for $N = L = 7$ with different crowding parameter between $C = [2, 3)$. The states with the largest PR value are in the first row ((a), (b), (c)), the states with the lowest PR are in the second row. The blue line is the smoothed survival probability averaged over 40 realizations of the disorder parameter, the analytic expression is shown as red line. Inside: the average LDoS of the corresponding state

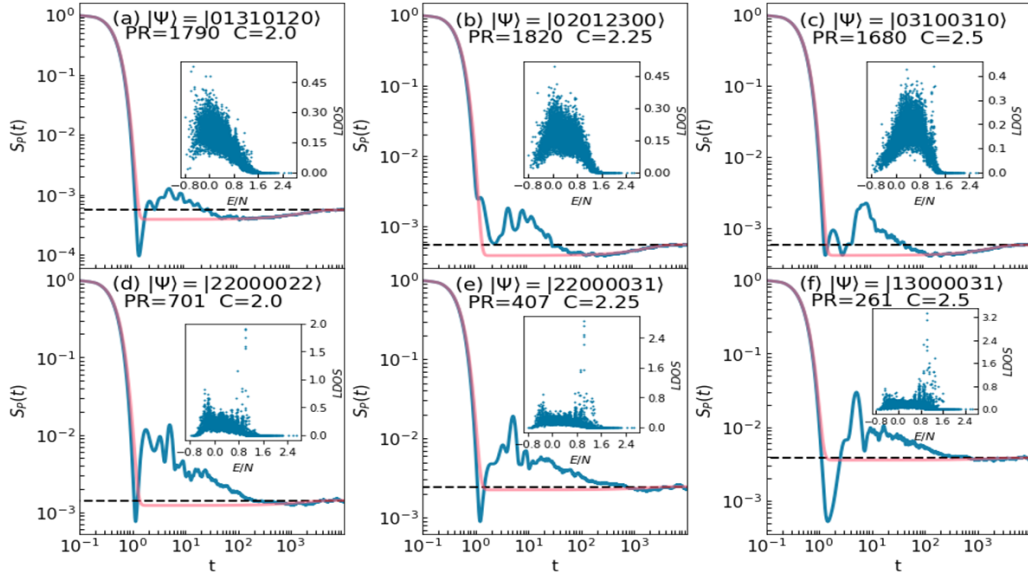


Figure 6: Survival probability of selected states for $N = L = 8$ with different crowding parameter between $C = [2, 3)$. The states with the largest PR value are in the first row ((a), (b), (c)), the states with the lowest PR are in the second row. The blue line is the smoothed survival probability averaged over 40 realizations of the disorder parameter, the analytic expression is shown as red line. Inside: the average LDoS of the corresponding state.

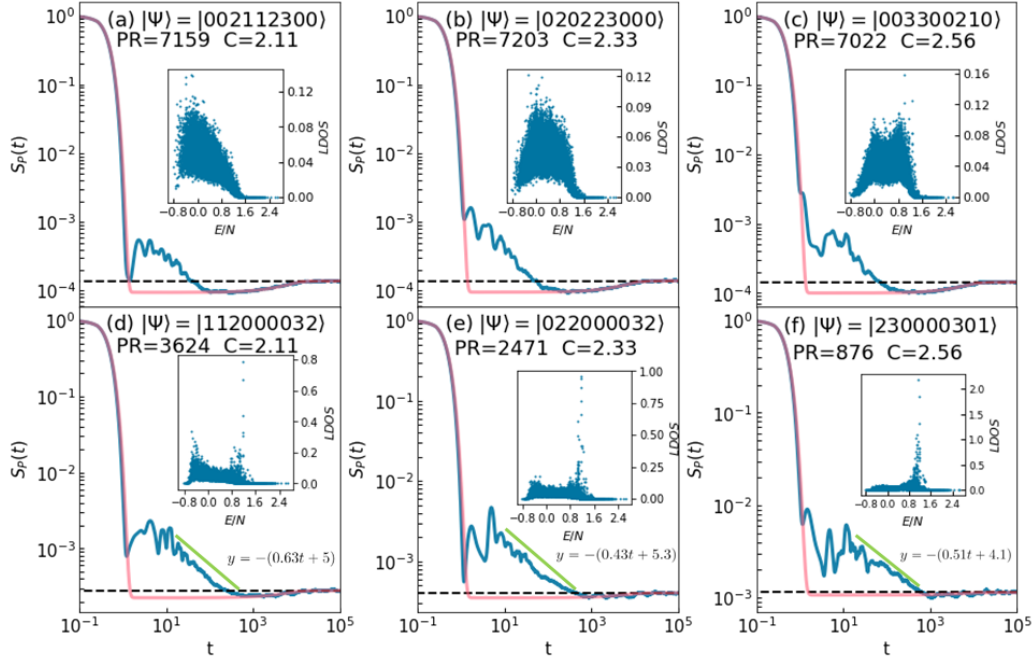


Figure 7: Survival probability of selected states for $N = L = 9$ with different crowding parameter between $C = [2, 3)$. The states with the largest PR value are in the first row (a), (b), (c), the states with the lowest PR are in the second row (d), (e), (f). The blue line is the smoothed survival probability averaged over 40 realizations of the disorder parameter, the analytic expression is shown as red line. Inside: the average LDoS of the corresponding state. Green lines in the bottom panels depict the power-law decay of the survival probability, whose exponent is given by the slope of the linear fits also shown next to the lines.

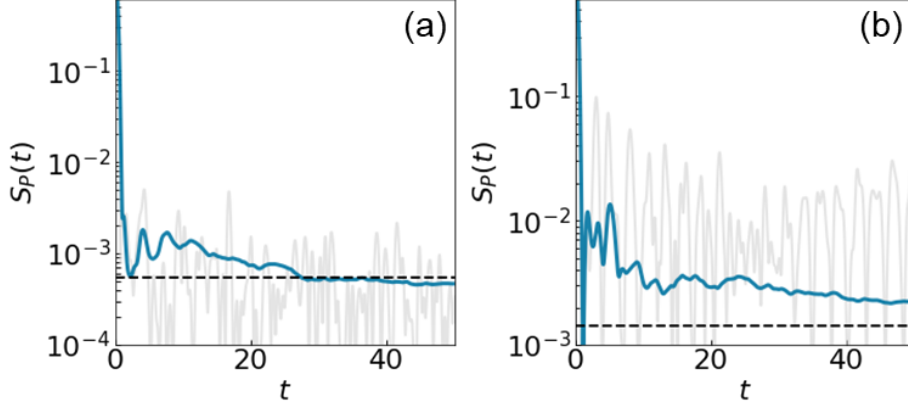


Figure 8: (a) Survival probabilities for the state $|\Psi(0)\rangle = |0, 2, 0, 1, 2, 3, 0, 0\rangle$ with high PR and (b) for a state $|\Psi(0)\rangle = |2, 2, 0, 0, 0, 0, 2, 2\rangle$, with low PR. In both cases for $N = L = 8$. The gray line corresponds to one random realization in ϕ and the blue line is the average over 40 realizations. These two states are the same considered in Fig.6(b) and (d), respectively.

behaviours of the whole basis, 6 initial states of the Fock basis with three different values of the crowding parameter C in the interval $C = [2, 3]$. For given system size and C , we consider a pair of states, one with the highest PR and a second one with the lowest PR (in Appendix B, for $N = L = 8$, results for states with intermediate values of the PR are presented). This allows us to contrast the differences in the behaviour of the SP. Varying randomly ϕ , we consider 40 realizations of the Hamiltonian for each initial state. We perform the same average over realizations and the same rolling temporal average as in Fig.4 (a) to obtain the results shown by blue lines in Figs. 5, 6 and 7 for $N = L = 7, 8$, and 9, respectively. In all these figures, we also plot with a red line the analytical expression of Eq.(13).

In all cases (Figs. 5, 6, and 7), the initial decay of the survival probability is Gaussian and adequately described by the red lines obtained from the squared magnitude of the Fourier transform,

eq.(14), of the smoothed LDoS which is also Gaussian. Likewise, in all cases the asymptotic value of the SP is given by the IPR, which is attained at very long times. Important differences in the behaviour of the SP can be observed at intermediate temporal scales.

After the initial Gaussian decay, the survival probability of all the states display a non-generic behavior, with oscillations whose amplitudes seem to decay according to a power-law [37] (see green lines in bottom panels of Fig. 7). At this scale, the analytical red lines do not describe, not even approximately, the numerical results. The origin of this behavior can be traced back to the details of the components of the initial state in the eigenbasis, the LDoS, whose averages over the 40 realizations are shown as insets in all the panels of the figures.

The main differences in the behaviour of the SP comes after the end of this power-law-decay regime. For states with large PR (upper row in figures 5, 6, and 7), the power-law regime ends at the bottom of the correlation hole that is clearly visible in the numerical (blue) lines and analytical (red) lines. From this time up to equilibration the numerical SP is very well described by the analytical expression and behaves according to the GOE correlations in the spectrum. For these states with large PR , the numerical SPs exhibit a ramp towards the asymptotic value that corresponds to the final stage of the correlation hole. Correspondingly, for these high- PR states we can observe a very dense LDoS in which all the Hamiltonian eigenstates in the chaotic region ($E/N \in [-0.4, 1]$) participate. The correlation hole ends at $t \approx 10^3$ for $N = 7$, at $t \approx 10^{3.5}$ for $N = 8$, and for $N = 9$ it ends at $t \approx 10^4$, which is approximately the corresponding Heisenberg time for each case, $t_H \propto \frac{\dim}{N}$.

On the other hand, for states with low PR (bottom row in all figures 5, 6 and 7) the survival probability behave very differently respect to the states with high PR, although all of them are in the chaotic region where ETH and RMT is valid. There are two main features in the survival probability differentiating their behaviour. The first one is that, for low-PR states, the power-law-decay regime persists for a longer time and ends at a time approximately one order of magnitude longer than in the states with large PR. The second one is that, for low-PR states, this power-law regime ends directly at the asymptotic value and a barely identifiable or even absent correlation hole is obtained for the SP of these states. The presence of the power law decay is illustrated in Figs. 7 (d,e,f), where a diagonal green straight line is plotted parallel to the peaks of the SP, with a slope 0.5 ± 0.1 . It means that in this temporal region, the survival probability of these states decays approximately as $t^{1/2}$.

The averaged LDoS display differences as well. In the insets of the panels for states with low PR (lower row in the figures), it can be observed that a small number of eigenstates have very large components, which explains the anomalous behaviour of the survival probability and the low PR of these states. It is worth noting the similarities of these low-PR states with the so-called many-body scarred states reported in other models [6, 7, 9, 38, 11, 12, 13, 15]. The scarred states are characterized by displaying persistent, long lasting revivals, the participation of a small set of eigenstates, which keep them trapped in a small, low entropy subspace which do not thermalize [15]. As a consequence, they do not display a correlation hole in their survival probability. In this model, another interesting property of these low-PR states is that initially the bosons are more concentrated near the borders

of the linear chain, with the middle sites empty. This suggests a connection between persisting revivals and boundary effects. A comparative study between the case studied here with the case of periodic boundary conditions would permit to establish this possible connection.

Finally, in order to unveil the properties of the SP that produce the power-law decay obtained in the ensemble average of the SP, both for states with high and low PR, in Fig. 8 we show the SP of two representative initial states, one with high PR and another one with low PR. Differently to previous figures, here we show the SP for only one realization of the Hamiltonian and use a linear scale in the horizontal time axis. We can see that in the case of the high-PR state we obtain revivals appearing randomly, whereas for the state with low PR the revivals are periodic and persists for a longer time, reinforcing the ideas that these low-PR states are scarred states.

5. Conclusions

We have presented a detailed study of the dynamics of states in the occupation basis under unitary evolution in the Interacting Aubry-André model, which has been recently realized experimentally, showing evidence of thermalization for the Mott state, which is a particular element of the occupations basis. For different number of particles (N) and sites (L), we have studied the spectral signatures of chaos, confirming that the system becomes chaotic when the disorder parameter W is small compared with the other Hamiltonian parameters. The system exhibits chaos in an intermediate energy per particle interval, being regular in the low and high energy extreme of the spectrum. We have verified that this energy per particle interval is approximately the same

for the three different system sizes considered $N = L = 7, 8$, and 9 , which have Hilbert space dimensions varying in one order of magnitude, from 1.7×10^3 up to 2.4×10^4 .

We have identified states of the occupation basis that show an anomalous behaviour in their dynamics. These states show lasting revivals and, although their energy components are located in the already identified chaotic region of the model, they do not show in their dynamics signatures of the correlated energy spectrum. These states have a low participation ratio of the energy components. On the contrary, states with large values of the participation ratio manifest the random-matrix correlations of the energy spectrum in their dynamics, in the form of a correlation-hole in their survival probability.

The states with low participation ratio and anomalous behaviour in their dynamics have similar characteristics as the so-called quantum scarred states, namely, lasting revivals and absence of a correlation-hole in the dynamics of their survival probability.

Additionally, we identified the closeness of the initial atoms to the border of the chain of sites as the origin of occupation states with small PR and anomalous dynamics. A comparison of the behaviour of the open chain studied here with a chain with periodic conditions would shed light about the possible relation between states with persisting revivals and border effects.

Acknowledgments: We acknowledge the support of the Computation Center - ICN, in particular to Enrique Palacios, Luciano D  az, and Eduardo Murrieta. This research was funded in part by the DGAPA- UNAM project number IN109523.

Competing interests: the authors have no competing interests to declare.

Credit roles: **Carlos Diaz Mejía:** Formal analysis, Software, Visualization, Writing - original draft, **Javier de la Cruz:** Formal analysis, Software, Visualization,

Sergio Lerma-Hernández: Conceptualization, Formal analysis, Writing - review & editing, **Jorge G. Hirsch:** Conceptualization, Formal analysis, Writing - review & editing.

Appendix A. Effective dimension and survival probability at short times

One of the parameters of the survival probability is the effective dimension η . The numerical estimation of η requires an integral involving the LDoS of a given state and the DOS of the whole system,

$$\eta = \frac{1}{\int dE \frac{\rho^2(E)}{\nu(E)}}. \quad (\text{A.1})$$

We explored performing the above integral in two different ways: approximating the Dirac deltas in the LDoS, $\rho_L(E)$, by Gaussian distributions of width ΔE , or performing a Riemann Sum with energy intervals given by ΔE . We found that the Riemann Sum shows less dispersion in the estimation of the η parameter.

To select the most convenient energy interval ΔE for performing the integral as a Riemman sum, we calculated η for $\Delta E \in [0.2, 1.8]$ for the state (a) $|\Psi(0)\rangle = |022000220\rangle$ and (b) $|\Psi(0)\rangle = |11111111\rangle$ considering 40 realizations in ϕ . For the first state, we obtain a value of $\eta = 5960 \pm 85$, whereas for the second state we obtained 3960 ± 30 , for $\Delta E \in [0.3, 1.8]$. These average values are shown as red lines in Fig. A.9. Both averages correspond to a $\Delta E = 0.74$. In this way, we are confident that the selected value

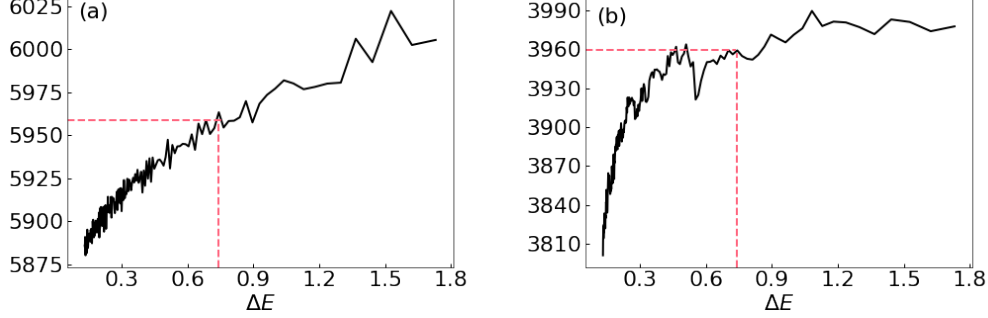


Figure A.9: η vs ΔE for the state (a) $|\Psi(0)\rangle = |022000220\rangle$ and (b) $|\Psi(0)\rangle = |11111111\rangle$ for 40 realizations in ϕ , the red lines are the values chosen in the numerical calculation, both corresponds to a $\Delta E = 0.74$

of η would not vary in more than 2% if we would have employed a different energy interval ΔE .

At short times, when the revivals have vanished and the correlation hole starts, the averaged survival probability has its lowest value along the ramp which will end at long times in the IPR. This bottom value is [34]

$$SP_{low} \approx IPR - \frac{1}{\eta}. \quad (\text{A.2})$$

This expression shows that the maximum depth of the correlation hole, below its asymptotic value, is $\frac{1}{\eta}$.

As the maximum depth of the correlation hole is $1/\eta$ below the asymptotic value $IPR = 1/PR$, it is interesting to know the relationship between these two quantities. In Fig. A.10 we show a plot of η vs PR , with the color code depicting the value of C , for all the states in the occupation basis, for a system of $N = 8$ bosons in $L = 8$ sites. For those states with PR values smaller than 400, which have the largest values of C and highest energies, η grows linearly with PR, with a relation close to $\eta \approx 10PR$. For states

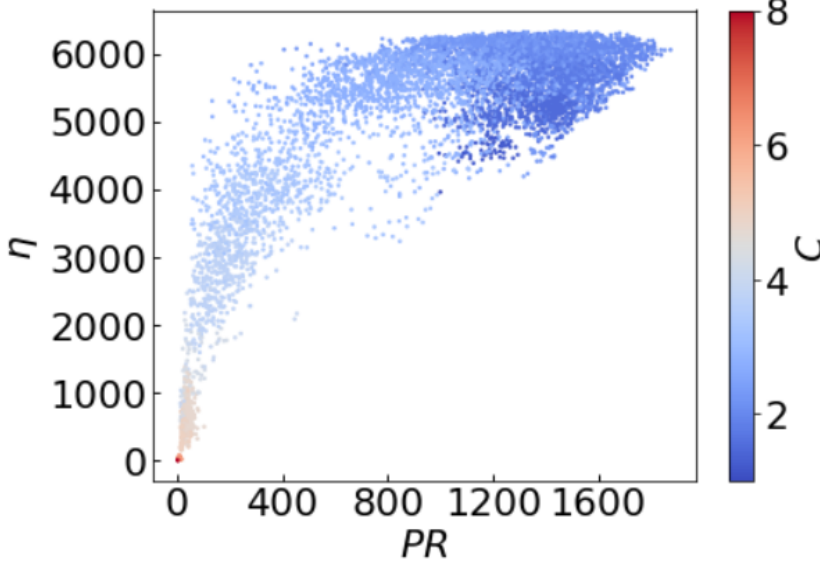


Figure A.10: η vs PR of each initial state vs C for 40 realizations in ϕ

in the low energy and chaotic region, $C \leq 4$, most of the states with $PR > 800$ have a nearly constant value $5000 < \eta < 6000$.

Appendix B. Emerging of the correlation hole.

In this section we describe how the correlation hole starts to appear for a specific value of the crowding parameter in the case $N = L = 8$. Figures B.11 ($C = 2.25$) and B.12 ($C = 2.5$) displays how the survival probability evolves as the PR increases.

We can observe that states with the lowest PR have no correlation hole and their SP shows a polynomial decay that persists until attaining its equilibration value. Their LDoS show as well shows large concentration in few eigenstates. In states with increasing PR the LDoS starts to be distributed along the eigenstates and the correlation hole emerges. It is noticeable that only a small set of states lacks of correlation hole, and that for these states the

bosons tend to be on the borders of the chain.

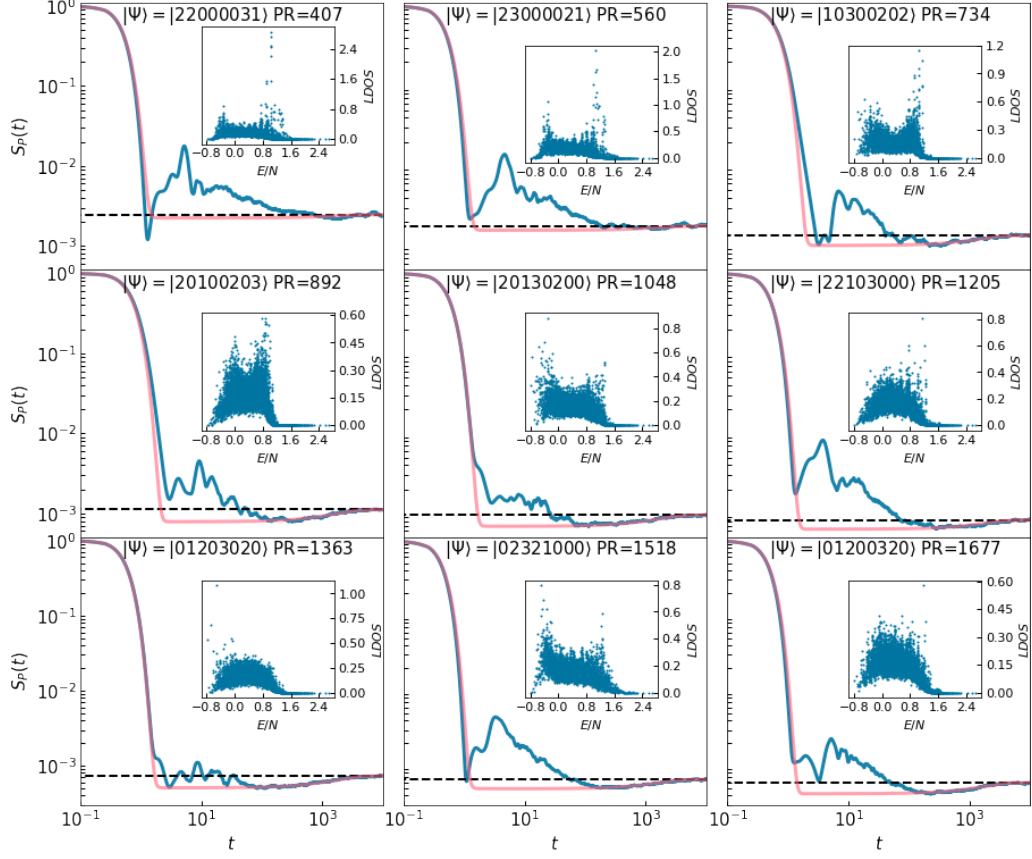


Figure B.11: Set of survival probabilities for $N = L = 8$ and $C = 2.25$. They are shown from its lowest $PR = 407$ up to $PR = 1677$ at constant steps. Inset: averaged LDoS of the corresponding state

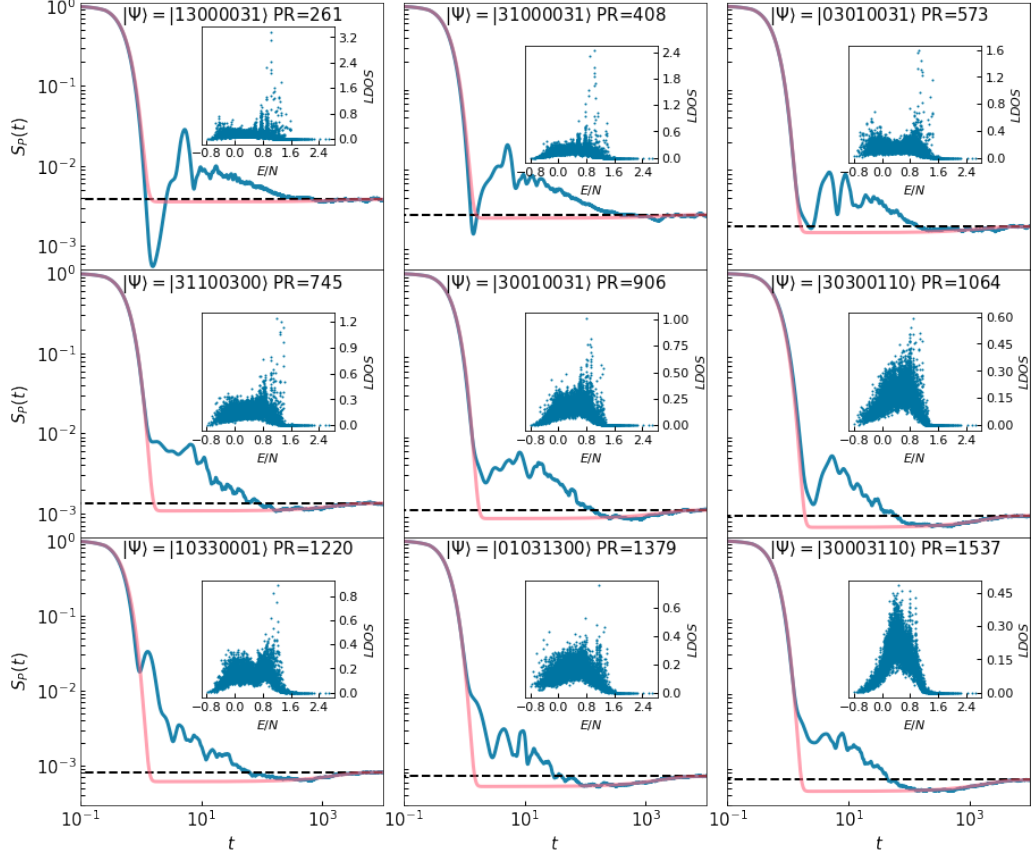


Figure B.12: Set of survival probabilities for $N = L = 8$ and $C = 2.5$. They are shown from its lowest $PR = 261$ up to $PR = 1537$ at constant steps. Inset: averaged LDoS of the corresponding state

References

- [1] O. Bohigas, M. J. Giannoni, and C. Schmit. Characterization of chaotic quantum spectra and universality of level fluctuation laws. Phys. Rev. Lett., 52:1–4, Jan 1984.
- [2] Michael Victor Berry, M. Tabor, and John Michael Ziman. Level clustering in the regular spectrum. Proceedings of the Royal Society of London. A. Mathematical and Physical Sciences, 356(1686):375–394, 1977.
- [3] Chaitanya Murthy and Mark Srednicki. Bounds on chaos from the eigenstate thermalization hypothesis. Phys. Rev. Lett., 123:230606, Dec 2019.
- [4] Mark Srednicki. Chaos and quantum thermalization. Phys. Rev. E, 50:888–901, Aug 1994.
- [5] Alexander Lukin, Matthew Rispoli, Robert Schittko, M. Eric Tai, Adam M. Kaufman, Soonwon Choi, Vedika Khemani, Julian Léonard, and Markus Greiner. Probing entanglement in a many-body-localized system. Science, 364(6437):256–260, 2019.
- [6] Maksym Serbyn, Dmitry A. Abanin, and Zlatko Papić. Quantum many-body scars and weak breaking of ergodicity. Nature Physics, 17(6):675–685, 2021.
- [7] Anushya Chandran, Thomas Iadecola, Vedika Khemani, and Roderich Moessner. Quantum many-body scars: A quasi-particle perspective. Annual Review of Condensed Matter Physics, 14:443–469, 2023.
- [8] Hannes Bernien, Sylvain Schwartz, Alexander Keesling, Harry Levine, Ahmed Omran, Hannes Pichler, Soonwon

- Choi, Alexander S Zibrov, Manuel Endres, Markus Greiner, et al. Probing many-body dynamics on a 51-atom quantum simulator. Nature, 551(7682):579–584, 2017.
- [9] CJ Turner, AA Michailidis, DA Abanin, Maksym Serbyn, and Z Papić. Quantum scarred eigenstates in a rydberg atom chain: Entanglement, breakdown of thermalization, and stability to perturbations. Physical Review B, 98(15):155134, 2018.
- [10] Soonwon Choi, Christopher J Turner, Hannes Pichler, Wen Wei Ho, Alexios A Michailidis, Zlatko Papić, Maksym Serbyn, Mikhail D Lukin, and Dmitry A Abanin. Emergent su(2) dynamics and perfect quantum many-body scars. Physical review letters, 122(22):220603, 2019.
- [11] Ana Hudomal, Ivana Vasić, Nicolas Regnault, and Zlatko Papić. Quantum scars of bosons with correlated hopping. Communications Physics, 3(1):99, 2020.
- [12] Quirin Hummel, Klaus Richter, and Peter Schlagheck. Genuine many-body quantum scars along unstable modes in bose-hubbard systems. Physical Review Letters, 130(25):250402, 2023.
- [13] Shane Dooley and Graham Kells. Enhancing the effect of quantum many-body scars on dynamics by minimizing the effective dimension. Physical Review B, 102(19):195114, 2020.
- [14] Henning Labuhn, Daniel Barredo, Sylvain Ravets, Sylvain De Léséleuc, Tommaso Macrì, Thierry Lahaye, and Antoine Browaeys. Tunable two-dimensional arrays of single rydberg atoms for realizing quantum ising models. Nature, 534(7609):667–670, 2016.

- [15] Guo-Xian Su, Hui Sun, Ana Hudomal, Jean-Yves Desaulles, Zhao-Yu Zhou, Bing Yang, Jad C Halimeh, Zhen-Sheng Yuan, Zlatko Papić, and Jian-Wei Pan. Observation of many-body scarring in a bose-hubbard quantum simulator. Physical Review Research, 5(2):023010, 2023.
- [16] G A Domínguez-Castro and R Paredes. The aubry–andré model as a hobbyhorse for understanding the localization phenomenon. European Journal of Physics, 40(4):045403, jun 2019.
- [17] A. R Kolovsky and A Buchleitner. Quantum chaos in the bose-hubbard model. Europhysics Letters (EPL), 68(5):632–638, dec 2004.
- [18] Corinna Kollath, Guillaume Roux, Giulio Biroli, and Andreas M Läuchli. Statistical properties of the spectrum of the extended bose–hubbard model. Journal of Statistical Mechanics: Theory and Experiment, 2010(08):P08011, aug 2010.
- [19] Javier de la Cruz, Sergio Lerma-Hernández, and Jorge G. Hirsch. Quantum chaos in a system with high degree of symmetries. Phys. Rev. E, 102:032208, Sep 2020.
- [20] J M Zhang and R X Dong. Exact diagonalization: the bose–hubbard model as an example. European Journal of Physics, 31(3):591–602, apr 2010.
- [21] Hans-Jürgen Stöckmann. Quantum chaos: an introduction, 2000.
- [22] Vadim Oganesyan and David A. Huse. Localization of in-

- teracting fermions at high temperature. Phys. Rev. B, 75:155111, Apr 2007.
- [23] N.D. Chavda, H.N. Deota, and V.K.B. Kota. Poisson to goe transition in the distribution of the ratio of consecutive level spacings. Physics Letters A, 378(41):3012–3017, 2014.
 - [24] Eduardo Jonathan Torres-Herrera and Lea F. Santos. Dynamical detection of level repulsion in the one-particle aubry-andré model. Condensed Matter, 5(1), 2020.
 - [25] Y. Y. Atas, E. Bogomolny, O. Giraud, and G. Roux. Distribution of the ratio of consecutive level spacings in random matrix ensembles. Phys. Rev. Lett., 110:084101, Feb 2013.
 - [26] Shashi C L Srivastava, Arul Lakshminarayan, Steven Tomsovic, and Arnd Bäcker. Ordered level spacing probability densities. Journal of Physics A: Mathematical and Theoretical, 52(2):025101, dec 2018.
 - [27] E. Brézin and S. Hikami. Spectral form factor in a random matrix theory. Phys. Rev. E, 55:4067–4083, Apr 1997.
 - [28] Y. Alhassid and R. D. Levine. Spectral autocorrelation function in the statistical theory of energy levels. Phys. Rev. A, 46:4650–4653, Oct 1992.
 - [29] E. J. Torres-Herrera and Lea F. Santos. Extended nonergodic states in disordered many-body quantum systems. Annalen der Physik, 529(7):1600284, 2017.
 - [30] E. J. Torres-Herrera and Lea F. Santos. Dynamical manifestations of quantum chaos: correlation hole and bulge. Philosophical Transactions of the Royal

Society A: Mathematical, Physical and Engineering Sciences, 375(2108):20160434, 2017.

- [31] E. J. Torres-Herrera, Antonio M. García-García, and Lea F. Santos. Generic dynamical features of quenched interacting quantum systems: Survival probability, density imbalance, and out-of-time-ordered correlator. Phys. Rev. B, 97:060303, Feb 2018.
- [32] Eduardo Jonathan Torres-Herrera and Lea F. Santos. Signatures of chaos and thermalization in the dynamics of many-body quantum systems. The European Physical Journal Special Topics, 227(15):1897–1910, Mar 2019.
- [33] Mauro Schiulaz, E. Jonathan Torres-Herrera, and Lea F. Santos. Thouless and relaxation time scales in many-body quantum systems. Phys. Rev. B, 99:174313, May 2019.
- [34] S. Lerma-Hernández, D. Villaseñor, M. A. Bastarrachea-Magnani, E. J. Torres-Herrera, L. F. Santos, and J. G. Hirsch. Dynamical signatures of quantum chaos and relaxation time scales in a spin-boson system. Phys. Rev. E, 100:012218, Jul 2019.
- [35] Olivier Giraud, Nicolas Macé, Éric Vernier, and Fabien Alet. Probing symmetries of quantum many-body systems through gap ratio statistics. Phys. Rev. X, 12:011006, Jan 2022.
- [36] D Villaseñor, S Pilatowsky-Cameo, M A Bastarrachea-Magnani, S Lerma-Hernández, L F Santos, and J G Hirsch. Quantum vs classical dynamics in a spin-boson system: manifestations of spectral correlations and scarring. New Journal of Physics, 22(6):063036, jun 2020.

- [37] Marco Távora, E. J. Torres-Herrera, and Lea F. Santos. Inevitable power-law behavior of isolated many-body quantum systems and how it anticipates thermalization. Phys. Rev. A, 94:041603, Oct 2016.
- [38] Cheng-Ju Lin and Olexei Motrunich. Exact quantum many-body scar states in the rydberg-blockaded atom chain. Physical Review Letters, 122, 04 2019.